nature portfolio

Peer Review File

Operating a non-Hermitian atomic magnetometer with programmable digital electronics

Corresponding Author: Professor Hui Jing

This file contains all reviewer reports in order by version, followed by all author rebuttals in order by version.

Version 0:

Reviewer comments:

Reviewer #1

(Remarks to the Author)
In the manuscript entitled "Operating a non-Hermitian atomic magnetometer with programmable digital electronics," the authors investigate a non-Hermitian system formed by hybridizing digital electronics with atomic sensors. The programmability of digital electronics enables exceptional points (EPs) to be created, manipulated, and applied easily and flexibly. They achieved a 4.27-fold enhancement in sensitivity for weak magnetic field measurements.
Non-Hermitian physics is currently a highly prominent research field, and studies on its practical applications are of great significance. This paper offers an excellent perspective: by constructing a hybrid system, it combines the respective advantages of both components to realize effective control and utilization of non-Hermitian properties, which is likely to inspire numerous new applications. In conclusion, I recommend the paper for publication.
Below are specific comments and suggestions:
1. In Fig. 3a, enhancement factors for g2 in the range 1 to 3 are plotted. It appears that the optimal result is achieved at g2=1. What about results for g2<1? Could the performance be even better?
2. What is the theoretical prediction for the response enhancement under the parameters used in Fig. 3a?
3. What is the optimal magnetic field measurement sensitivity of the system?
4. What is the primary noise source of the system?
5. It is suggested that the authors cite relevant references on enhancing magnetic field measurement sensitivity using non-Hermitian properties, such as Phys. Rev. Lett. 130, 263601 (2023) and Phys. Rev. Lett. 130, 193602 (2023).
6. Please correct formatting errors, such as those in line 467.

Reviewer #3

(Remarks to the Author)
This manuscript presents a novel integration of digital electronics to generate an exceptional point in a Rb/Xe comagnetometer system, demonstrating enhanced magnetic field sensitivity by a factor of 4. The architecture is simple and seemingly applicable to other spin-based systems. Experimental evidence of EP behaviour is compelling, and the digital electronics package appears to be a powerful tool for atomic sensing.

However, the paper lacks many experimental and theoretical details, and lacks clarity in presentation, which I believe means that this paper requires major revisions before it can be reconsidered. It has taken many read-throughs of the paper to get a grasp of the setup and results, which I therefore think means it requires significantly more work to make it more readable.

The fact that the term comagnetometer is not being used to describe this system is somewhat puzzling. Admittedly, this approach can be used on a traditional atomic magnetometer (e.g. just Rb/N2 or Rb/paraffin), but it is used on a comagnetometer system here (Rb/Xe/(N2?)). In a comagnetometer (i.e. this system), you typically do not want to be sensitive to magnetic fields, you only want to be sensitive to rotations. This is why people typically use two Xe isotopes with opposite gyromagnetic ratios for rotation measurements. The authors should be much clearer about how they intend to use this comagnetometer, and what applications this enhanced sensitivity to magnetic fields will be, because my understanding is that this will worsen the comagnetometer’s performance as a gyroscope.

Readability of theory:
- To me, the derivation in the supplementary material is a critical part of the manuscript, and shows how a set of coupled

differential equations (dy1/dt = … Eq. 6 in supplementary and dy2/dt=… Eq. 10 in supplementary) are solved to find the eigenvalues λ. There is so little detail given in the manuscript about how Eq. 1 is derived that the reader must go to the supplementary material to see the derivation. I also don't think calling it a Hamiltonian is necessarily the best terminology, as this implies some sort of quantum nature of the digital electronics package, when in fact the authors are just solving two coupled differential equations (dM/dt for the atomic spins and dy/dt for the digital electronics package). I was very confused to begin with as thought this was discussing some energy level system.

- Eq. 2 is also very unclear in the manuscript as it looks dimensionally incorrect (I know you've set g=k=1). Also, substituting θ=π/2 into Eq. 1 gives -i, not +i, which makes me a bit critical about what's being plotted in Fig. 2d given these mistakes.
- I would strongly recommend re-writing the theory section of this paper to make it much clearer, akin to the approach taken in the supplementary material. There is no mention in the main text that you're using Bloch equations to describe your atomic spins. Minor thing but I would use Δv for frequency difference. The authors should also define all variables in much greater detail providing units (e.g. k1, k2, g1, g2 are all gains but should have units included).

Figures:

- Fig. 1: In Fig. 1b the y-label is 'Non-EP response' which I presume should be the frequency of Xe, but is unclear. The x-axis is v, which is strange to use as this is the detuning between the frequency of the digital resonator and the Larmor frequency of Xe, so presumably this should just be the Larmor frequency of Xe. In Fig. 1c the y-axis should again be frequency of the Xe and frequency of the digital resonator. The fact it's not written like this makes it difficult to understand what's happening in the graphs. The graphs in Fig. 1d make more sense. It shows that the Xe co-magnetometer is more sensitive to shifts of DC magnetic fields. This nicely shows how near the exceptional point the Xe is more sensitive to magnetic fields. The purpose of the data in Fig. 1d(ii) is unclear, as it seems to show the same effect as in Fig. 1(d).
- Fig. 2: In Fig. 2(a) the signal should not be a FID - instead it should be a sine wave as this is in the feedback configuration. Fig. 2(b) is very confusing, as the x-axis seems to be centred around 100mHz. Presumably this data was taken with a bias field of 161.1Hz, and therefore this should either be centred around 161.1Hz (which I think is easier for the reader), or it should be centred around 0Hz if Δv is along the x-axis. I don't really understand the relevance of Fig. 2b(ii), as the Xe atoms are the sensor and therefore it is not clear to me why the addition is shown. The graphs in Fig. 2(d) are important and nicely done. The graphs show that Xe becomes more sensitive to magnetic fields, i.e. bigger frequency shift for small change in bias field. The theory and experiment overlap. But Voltage U (mV) is undefined in the text - I presume this is the current sent to the coil? Also, the y-axis should read frequency difference, or if it's frequency it should be 161.1 Hz. Parameters like g2, k2, U are used interchangeably without proper definitions

Lack of experimental details: The fact that the makeup of the vapour cell (Rb, Xe, N2?) is not included until the methods section is a big omission. Is there buffer gas in the Xe/Cs cell? What is the pressure in the cell? Move essential details of experimental setup (nitrogen pressure, Xe129 pressure, cell temperature, DE settings) into main text. No details are given about the DE package. Is this a DDS or FPGA? What settings are used? There is no chance for the reader to replicate what has been shown here experimentally. I would strongly encourage the authors to think about all the details that would be necessary to replicate this experiment, including lasers used (transition, powers) etc.

Missing key citation: 'Stable Atomic Magnetometer in Parity-Time Symmetry Broken Phase, Phys. Rev. Lett. 130, 023201 (2023)'. This is a great example of a paper where PT symmetry breaking is demonstrated in Xe129. They do systematic measurements of how magnetic field gradients induce PT symmetry breaking in Xe129 - the mechanism for how PT symmetry is broken is very clear, and is a good example of the clarity the authors should be aiming for in this paper.

Version 1:

Reviewer comments:

Reviewer #1

(Remarks to the Author)
The authors have carefully addressed all the previously raised comments and revised the manuscript accordingly. I recommend the acceptance of this manuscript.

Reviewer #3

(Remarks to the Author)
The authors of the paper have improve the readability of the figures and text in the manuscript, and I will therefore recommend this for publication.

We thank the reviewers for carefully reviewing our manuscript and highly recognizing the innovation of our work. We have carefully addressed all issues and accordingly optimized the manuscript content. The details are as follows:

Responses to the comments of Reviewer #1

Comment #1:

In the manuscript entitled "Operating a non-Hermitian atomic magnetometer with programmable digital electronics," the authors investigate a non-Hermitian system formed by hybridizing digital electronics with atomic sensors. The programmability of digital electronics enables exceptional points (EPs) to be created, manipulated, and applied easily and flexibly. They achieved a 4.27-fold enhancement in sensitivity for weak magnetic field measurements.

Non-Hermitian physics is currently a highly prominent research field, and studies on its practical applications are of great significance. This paper offers an excellent perspective: by constructing a hybrid system, it combines the respective advantages of both components to realize effective control and utilization of non-Hermitian properties, which is likely to inspire numerous new applications. In conclusion, I recommend the paper for publication.

Below are specific comments and suggestions:

1.In Fig. 3a, enhancement factors for g2 in the range 1 to 3 are plotted. It appears that the optimal result is achieved at g2=1. What about results for g2 <1? Could the performance be even better?

Response #1:

First, we thank you for your patient review and full recognition of our work. Your question about the system at $g_2 < 1$ is indeed a key point. Therefore, we have added supplementary explanations in the Methods section to avoid confusion for other readers on this point. When in the single-EP state, the system is strictly at the EP only when $g_2 = 1$. Thus, both continuously increasing and decreasing g_2 will cause the system to deviate from the EP, eventually leading to a continuous decrease in the response enhancement factor.

We would like to additionally note that in the original manuscript we set $g_1 = g_2 = 1$ and subsequently discussed the relative magnitude of g_2 and 1. In the latest version of the article, we set $g_1 = g_2 = g_0$ and discuss the magnitude relationship between g_2/g_0 and 1. This adjustment does not affect the theoretical and experimental results in the paper. The purpose of this adjustment is to better discuss the relationship between gain and loss in the Supplementary materials, and we hope it will provide a better reading experience.

We have made the following revisions to the manuscript:

(i) We have redefined $g_2/g_0 = 1$ (originally defined as $g_2 = 1$) to represent the system at the EPs, and discussed the magnitude of g_2/g_0 to explain the system's state when g_2/g_0 deviates from 1.

(ii) We have added a discussion in the Methods section regarding the trend of system response when $g_2/g_0 < 1$, thereby completing the theoretical details of gain control.

Revised content in the Methods:

Starting from the single-EP configuration, gain control can change the response characteristics of the system. When g_2/g_0 is no longer fixed at 1, the expression for the eigenvalues is as follows:

$$\lambda = \frac{1}{2}\left(-i\gamma_0 + ig_0 - ig_2 \pm \sqrt{(2\Delta\omega + ig_0 + ig_2)^2 + 4g_0g_2}\right). \tag{4}$$

By adjusting g_2, we shift the system away from the EP, modifying the response zero-crossing slope and linearity. The response enhancement is related to the slope of the real part of the eigenvalue:

$$\left.\frac{\partial\lambda(Re)}{\partial\omega}\right|_{(\Delta\omega=0)} = \left|\frac{g_0+g_2}{g_0-g_2}\right|. \tag{5}$$

According to this equation, when $g_2/g_0 > 1$ (or $g_2/g_0 < 1$), the response amplification decreases. When $g_2/g_0 \to +\infty$ (or $g_2/g_0 \to 0$), the slope of the real part of the eigenvalue approaches 1. Therefore, as g_2/g_0 increases (or decreases), the system response shifts from sublinear to linear, with linearity increasing gradually.

Comment #2:

What is the theoretical prediction for the response enhancement under the parameters used in Fig. 3a?

Response #2:

Thank you for your good question. Reference [Photonics Res. 8, 1457 (2020)] points out that when the system is at EPs, its theoretical prediction for the response enhancement can reach positive infinity. Under the conditions of Fig. 3a, our system is at EPs. Therefore, its enhancement should also be positive infinity.

However, in practice, the conditions to reach this limit are extremely stringent: noise-free operation, infinitesimal input, and the system remaining exactly at the EP throughout the sensing process. Therefore, intense ongoing efforts are made towards approaching this limit but currently it is still a challenge for experimentalists.

Comment #3:

What is the optimal magnetic field measurement sensitivity of the system?

Response #3:

Thank you for raising this good question. In the experiments in this paper, we use

$$NEM_B(f) = \frac{\sqrt{S_{out}(f)}}{\left|\frac{\partial s}{\partial B}\right| \cdot H(f)}$$

to measure the system's sensitivity. The sensitivity of the single atomic magnetometer and the EP-enhanced magnetometer for measuring a 0.05 Hz alternating magnetic field is approximately $42.23\ \mathrm{pT}/\sqrt{\mathrm{Hz}}$ and $9.89\ \mathrm{pT}/\sqrt{\mathrm{Hz}}$, with an improvement factor of about 4 times. This is comparable to the measurement results in reference [Phys. Rev. A 103, 053523 (2021)]. In this paper, the authors used a multipass cell to enhance ^{129}Xe 's sensitivity for rotation measurement, and the equivalent magnetic field measurement sensitivity is $10\ \mathrm{pT}/\sqrt{\mathrm{Hz}}$, representing an approximately 6-fold improvement compared to conventional cells. In addition, we have given more details about the relationship between sensitivity and SNR in the Supplementary materials. In our future works, we will make more efforts to further improve the sensitivity of our system (such as the index).

Revised content in the main text:

In the experiments of this work, we use the noise-equivalent magnetic field (NEM) to quantify the sensitivity. The sensitivity is related to the signal-to-noise ratio (SNR) by $\mathrm{NEM} \propto 1/\mathrm{SNR}$. Therefore, as shown in Fig. 3, we first measure the response and noise enhancement factors of the system, and then divide the former by the latter to obtain the SNR improvement factor, which is also the sensitivity enhancement factor of the system.

Revised content in the Supplementary materials:

When measuring the system's response at a specific frequency point, the Noise-Equivalent Magnetic field (NEM) needs to be introduced to define the sensitivity:

$$NEM_B(f) = \frac{\sqrt{S_{out}(f)}}{\left|\frac{\partial s}{\partial B}\right| \cdot H(f)},$$

where $\sqrt{S_{out}(f)}$ is the output noise amplitude spectral density, $\frac{\partial s}{\partial B}$ is the linear gain of the output signal with respect to the magnetic field, i.e., the system's response to the input signal. Since SNR is precisely the ratio of the response to the noise, the relationship between the $\sqrt{S_{out}(f)}/\left|\frac{\partial s}{\partial B}\right|$ term in the above equation and the SNR is:

$$\sqrt{S_{out}(f)}/\left|\frac{\partial s}{\partial B}\right| \propto \frac{1}{SNR}.$$

Then, $H(f)$ is the system's dynamic response given by $H(f) = \frac{1}{\sqrt{1+(f/f_c)^2}}$, where f_c

is the linewidth $\gamma/2\pi$. Since in the single-EP state the system loss does not change compared to the AM unit (as mentioned in the Supplementary materials), $H(f)$ is likewise an invariant. Finally, we obtain the relationship between system sensitivity and signal-to-noise ratio as $NEM_B(f) \propto 1/SNR$, which means sensitivity is inversely proportional to SNR.

Comment #4:

What is the primary noise source of the system?

Response #4:

For atomic magnetometers, noise is typically divided into three major categories: quantum noise, environmental noise, and technical noise. Specifically, the main component of system noise is the frequency estimation noise generated during the frequency measurement process, whose magnitude is directly determined by the system SNR and is affected by the shot noise level (see, e.g., Eur. Phys. J. D 57, 303 (2010)). The frequency estimation noise can be simultaneously classified as quantum noise and technical noise. Since the generation mechanism of it is independent of the input, it will not be further amplified during the EP enhancement process, which means it is part of N_a. Therefore, this noise will be suppressed during the EP-enhanced sensing process. This is also one of the reasons why we ultimately achieved an improvement in sensitivity measurement.

In our previous work, we have calibrated the magnetic field noise of this system, which is approximately $5-10\ \mathrm{pT}/\sqrt{\mathrm{Hz}}$ at 0.05 Hz (see, e.g., Chinese Phys. B 32, 040601). This noise belongs to N_I and will be amplified by the EP effect. Theoretically, this noise level represents the measurement limit of the EP-enhanced magnetometer. Since precise noise measurement is not the key innovation focus of this paper, more research on noise sources will be given further emphasis in our future work. To help readers better understand the noise characteristics of our system, we have provided more details about the noise source in the Methods section.

Revised content in the Methods:

The noise sources of an atomic magnetometer can be divided into three main categories: quantum noise, environmental noise, and technical noise. Quantum noise includes spin-projection noise, photon shot noise, and AC-Stark–shift–associated noise. In general, these all belong to N_a, i.e., the background noise. Environmental noise mainly consists of thermal noise and magnetic-field noise. In practical measurements, thermal noise is essentially independent of the signal strength to be measured and therefore belongs to N_a, whereas magnetic-field noise is amplified together with the signal after it is input into the system and thus belongs to N_I. Technical noise involves a wide variety of contributing factors, including laser, detector, electronic, and mechanical noise. These noises are distributed over all stages of the sensing process and are related to the hardware configuration. Consequently, part of them arises in the coupling stage of the system, and another part is introduced together with the input signal, contributing to N_a and N_I, respectively.

Comment #5:

It is suggested that the authors cite relevant references on enhancing magnetic field measurement sensitivity using non-Hermitian properties, such as Phys. Rev. Lett. 130, 263601 (2023) and Phys. Rev. Lett. 130, 193602 (2023).

Response #5:

Thank you for recommending two excellent and closely related papers. We have added them in the main text.

Comment #6:

Please correct formatting errors, such as those in line 467.

Response #6:

Thank you for your reminder. This error was caused by automatic PDF conversion when uploading the manuscript file. We have corrected it and will conduct targeted checks in subsequent steps to prevent similar errors.

Responses to the comments of Reviewer #2

Comment #1:

This manuscript presents a novel integration of digital electronics to generate an exceptional point in a Rb/Xe comagnetometer system, demonstrating enhanced magnetic field sensitivity by a factor of 4. The architecture is simple and seemingly applicable to other spin-based systems. Experimental evidence of EP behaviour is compelling, and the digital electronics package appears to be a powerful tool for atomic sensing.

However, the paper lacks many experimental and theoretical details, and lacks clarity in presentation, which I believe means that this paper requires major revisions before it can be reconsidered. It has taken many read-throughs of the paper to get a grasp of the setup and results, which I therefore think means it requires significantly more work to make it more readable.

The fact that the term comagnetometer is not being used to describe this system is somewhat puzzling. Admittedly, this approach can be used on a traditional atomic magnetometer (e.g. just Rb/N2 or Rb/paraffin), but it is used on a comagnetometer system here (Rb/Xe/(N2?)). In a comagnetometer (i.e. this system), you typically do not want to be sensitive to magnetic fields, you only want to be sensitive to rotations. This is why people typically use two Xe isotopes with opposite gyromagnetic ratios for rotation measurements.

Response #1:

Thank you for your very careful evaluation and constructive comments on our work.

First, we sincerely apologize for the lack of some experimental and theoretical details in the original version, and therefore we have rewritten the theoretical section and added sufficient experimental details (for details, see the revised manuscript and the corresponding contents in this response letter).

Next, regarding the terminology "comagnetometer": indeed, our research is based on the Rb-Xe spin system, which can cancel magnetic field fluctuations by separately measuring the precession frequencies of ^{87}Rb and ^{129}Xe, thereby functioning as a gyroscope to measure rotation signals. This method has been studied and demonstrated in [Sensors 12, 6331 (2012)] and [Rev. Sci. Instrum. 83, 103104 (2012)]. Additionally, ^{87}Rb and two Xe isotopes (^{129}Xe and ^{131}Xe) can also construct a comagnetometer system. As mentioned in the reference [Phys. Rev. Lett. 130, 023201 (2023)], this scheme utilizes the precession signals of Xe isotopes to measure rotation, while ^{87}Rb serves as a signal readout tool to measure the precession signals of ^{129}Xe and ^{131}Xe. So, in this sense, it is reasonable to use the terminology "comagnetometer".

However, we also understand that in some measurement scenarios, some researchers use noble gases to measure the magnetic field, while alkali metals serves as a signal readout tool. In such cases, the system is referred to as a "magnetometer" rather than a "comagnetometer". For example, in [EPJ Techniques and Instrumentation 1, 8 (2014)] and [EPJ D 73, 150 (2019)], the authors used ^{3}He to measure the magnetic field and used Rb as a zero-field magnetometer to measure the precession signal of ^{3}He. In these two papers, their measurement process is very similar to ours, even though they used two separate cells to encapsulate ^{3}He atoms and Rb atoms.

We also note that in our paper, our main purpose is to verify the advantages of digital resonators in constructing and controlling non-Hermitian hybrid systems. For this, we used Xe atoms in our experiment as part of the non-Hermitian system construction (i.e., the AM unit), while Rb atoms were only used for signal readout. Thus, the experimental process is more similar to the working process of the aforementioned "^{3}He magnetometer".

In fact, after verifying the non-Hermitian effects of Xe atoms, this system can be further developed into a comagnetometer to measure rotation (Since Xe atoms can be more sensitive in magnetic field measurement within the hybrid system, using them to construct a comagnetometer can likewise enhance the system's sensitivity to rotation. We have given the relevant derivation details in the response to the next review comment.). In our future works, we will expand our research results for more specific application scenarios.

In summary, we greatly appreciate the questions and suggestions you raised, which not only made us reconsider the definition of the system more carefully, but also reminded us that we need to provide a more comprehensive description of its potential applications. Therefore, we have added more content to the Discussion section to help readers to better understand these details.

Revised content in the Discussion:

Furthermore, although we have only demonstrated the sensitivity enhancement for magnetic field measurement by using ^{129}Xe, we believe that using the DE unit constructing other non-Hermitian spin sensors is also feasible. For example, coupling other atoms (such as ^{3}He, Cs, and Rb) with the DE unit can establish corresponding EP-enhanced magnetometers, which are expected to further improve the sensitivity of magnetic field measurement; coupling Xe isotopes (^{129}Xe and ^{131}Xe) with the DE unit can construct an EP-enhanced comagnetometer for improving the system's rotation measurement sensitivity. Overall, thanks to the flexible advantages of the DE unit, our technical solution can meet diverse application requirements.

Comment #2:

The authors should be much clearer about how they intend to use this comagnetometer, and what applications this enhanced sensitivity to magnetic fields will be, because my understanding is that this will worsen the comagnetometer's performance as a gyroscope.

Response #2:

Thank you again for reminding us to provide a more comprehensive explanation of the application prospects of this work. As mentioned in the previous response to the comment, we have added this content to the Discussion section.

Additionally, when near EPs, Xe's higher sensitivity allows it, in principle, to detect smaller rotation signals. This is because the essence of EP enhancement is to increase the slope of Xe's frequency response curve, so frequency shifts caused by either magnetic fields or rotation are amplified by this effect. Therefore, a tiny external rotation $\Delta\Omega$ causes a larger change in the eigenfrequency of ^{129}Xe.

We know that the precession frequency of atoms is affected by both magnetic field and rotation:

$$\omega_{Xe} = \Gamma_{Xe} B + \Omega,$$

where ω_{Xe} is the Larmor precession frequency of Xe, Γ_{Xe} is the gyromagnetic ratio, and B and Ω are the external magnetic field and rotation, respectively. Assuming that at the EPs, the frequency response slopes of Xe's two isotopes are enhanced by the factor of k_1 and k_2, we can obtain:

$$\Delta\omega_{129} = k_1(\Gamma_{129}\Delta B + \Delta\Omega),$$

$$\Delta\omega_{131} = k_2(\Gamma_{131}\Delta B + \Delta\Omega).$$

Here, $\Delta\omega_{129}$ and $\Delta\omega_{131}$ are the frequency shifts caused by external magnetic field and rotation disturbances (ΔB and $\Delta\Omega$). Based on the above equations, the solutions for magnetic field and rotation can be obtained respectively:

$$\Delta B = \frac{\Delta\omega_{129}/k_1 - \Delta\omega_{131}/k_2}{\Gamma_{129} - \Gamma_{131}}; \Delta\Omega = \frac{\Gamma_{131}\Delta\omega_{129}/k_1 - \Gamma_{129}\Delta\omega_{131}/k_2}{\Gamma_{131} - \Gamma_{129}}.$$

For convenience of discussion, we assume $k_1 = k_2 = k$. When measuring rotation, we first use the former formula to determine magnetic field fluctuations and compensate for them. At the EPs, since $k > 1$, a smaller magnetic field can be detected, although experimentally, it depends on higher-precision equipment. Then, when using the latter formula, smaller rotation changes can be measured, and the precision will be improved by k times. It means that after Xe's frequency response slope is amplified, although Xe becomes more sensitive to magnetic field disturbances, this also implies better magnetic compensation precision, thereby mitigating this disadvantage. While Xe's response to rotation is amplified by the same factor. When this advantage is preserved, EP-enhanced rotation measurement can theoretically be realized.

Admittedly, under current experimental conditions, we need to implement several upgrades (e.g., adding a rotation platform, magnetic compensation system and other equipment) before we can further investigate the non-Hermitian effects in rotation measurement. We will incorporate this research direction into our future plans and look forward to achieving new innovative results in our future works.

Comment #3:

Readability of theory:

To me, the derivation in the supplementary material is a critical part of the manuscript, and shows how a set of coupled differential equations (dy_1/dt = ... Eq. 6 in supplementary and dy_2/dt = ... Eq. 10 in supplementary) are solved to find the eigenvalues λ. There is so little detail given in the manuscript about how Eq. 1 is derived that the reader must go to the supplementary material to see the derivation.

Response #3:

Thank you for your suggestion. We sincerely apologize for the lack of theoretical details in the manuscript. We have decided to rewrite the theoretical section of the main text according to your proposed standards, adding appropriate formula derivation details.

We ultimately made the following adjustments to the theoretical section of the main text:

(i) We have added the derivation process from the Bloch equations and harmonic resonator differential equations to the Hamiltonian in the main text.

(ii) We have added the explanation of the system's physical quantities in the main text.

(iii) We have added the explanation of Ψ and $\hat{H}_{eff}$ in the main text.

Revised content in the main text:

The AM unit in the system can be described by the Bloch equations:

$$\dot{M}_x = \omega_y M_z - \omega_z M_y - M_x/T_2,$$

$$\dot{M}_y = \omega_z M_x - \omega_x M_z - M_y/T_2, \tag{1}$$

$\dot{M}_z = \omega_x M_y - \omega_y M_x - (M_0 - M_z)/T_1$.

Where $M_{x,y,z}$ are the projections of the atomic magnetization vector $\vec{M}$ on the x, y and z axes, $\omega_{x,y,z} = \Gamma B_{x,y,z}$ is the atomic precession frequency about the x, y and z axes, and Γ is the atomic gyromagnetic ratio, T_1 and T_2 are the longitudinal and transverse relaxation times of the atom, respectively. We denote $y_1 = M_+ = M_x - iM_y = M_\perp \cdot e^{i\varphi}$ as the signal output of the atoms, and $x_1 = M_z\, \omega_x = M_z\, \Gamma B_x$ as the signal input caused by the magnetic field B_x from the x-axis coil. Here, $\omega_z = \omega_1$ represents the eigenfrequency of atomic precession, $1/T_2 = \gamma_1$ indicates the loss, and $\omega_y = 0$ signifies no input along the y-axis. Assuming M_z remains constant during the experiment, equation (1) can be rewritten as follows:

$$\dot{y_1} = -(i\omega_1 + \gamma_1)y_1 + ix_1. \quad (2)$$

The DE unit is a one-dimensional digital resonator simulated by a computer, which can be described by the following differential equation:

$$\ddot{y_2} + 2\gamma_2\dot{y_2} + \omega_2^2 y_2 = 2\gamma_2\omega_2 x_2, \quad (3)$$

here, x_2 and y_2 represent the input and output of DE unit, ω_2 is the eigenfrequency, and γ_2 is the loss. After applying approximation and order reduction to Eq. (3), we obtain:

$$\dot{y_2} = -(i\omega_2 + \gamma_2)y_2 + ix_2. \quad (4)$$

Next, as shown in Fig. 1(a), we linearly add their outputs and use the result as the system input, thus obtaining $x_n = g_n(\kappa_1 e^{-i\theta} y_1 + \kappa_2 e^{-i\varphi} y_2)$. Here $e^{-i\theta}$ and $e^{-i\varphi}$ are phase-shift factors and κ_1, κ_2, g_1, and g_2 are gain factors, all of which can be tuned in the computer simulation. Finally, by defining $\Psi = (y_1\ y_2)^{\mathrm{T}}$, the system of equations can be written in a Schrödinger-like form, namely $\dot{\Psi} = -iH_{eff}\Psi$, where the effective Hamiltonian is given by:

$$\hat{H}_{eff} = \begin{bmatrix} \Delta\omega - i\gamma_1 - g_1\kappa_1 e^{-i\theta} & -g_1\kappa_2 e^{-i\varphi} \\ -g_2\kappa_1 e^{-i\theta} & -\Delta\omega - i\gamma_2 - g_2\kappa_2 e^{-i\varphi} \end{bmatrix}, \quad (5)$$

where $\Delta\omega$ is the eigenfrequency difference between atoms and the digital resonator. Additionally, the Hamiltonian contains phase shift factors $e^{-i\theta}$ and $e^{-i\varphi}$ and gain factors κ_1, κ_2, g_1, and g_2. Similarly, the eigenvalues contain these parameters, providing a diverse way to generate and control the hybrid EPs. Changing B_z alters the atomic eigenfrequency, and adjusting the phase and gain modules alters the gain and energy exchange of the hybrid system, which is crucial for controlling the hybrid EPs.

Comment #4:

I also don't think calling it a Hamiltonian is necessarily the best terminology, as this implies some sort of quantum nature of the digital electronics package, when in fact the authors are just solving two coupled differential equations (dM/dt for the atomic spins and dy/dt for the digital electronics package). I was very confused to begin with as thought this was discussing some energy level system.

Response #4

In many EP sensing-related literatures, authors frequently use the effective Hamiltonian H_{eff} to describe the evolution of the system, even though these systems are no longer limited to quantum systems as stated by the Reviewer. For a better description of our system, as inspired by the Reviewer and some nice works such as [Phys. Rev. Lett. 123, 213901 (2019)], [Phys. Rev. Lett. 130, 263601 (2023)], [APL Photonics 8, 036112 (2023)], [Science Advances 10, eadl5037 (2024)] and [Nat. Nanotechnol. 19, 1729 (2024)], we have redefined the amplitude of the dual harmonic resonator as $\Psi = (y_1\ y_2)^{\mathrm{T}}$. This approach allows the resonator's equation of motion to be treated as a Schrödinger-like equation, and the coefficient matrix obtained is the effective Hamiltonian H_{eff} (see also the above references).

Comment #5:

I would strongly recommend re-writing the theory section of this paper to make it much clearer, akin to the approach taken in the supplementary material. There is no mention in the main text that you're using Bloch equations to describe your atomic spins. Minor thing but I would use $\Delta\nu$ for frequency difference. The authors should also define all variables in much greater detail providing units (e.g. k1, k2, g1, g2 are all gains but should have units included).

Response #5:

Following your nice suggestions, we have given more details in the theoretical section. Also, when reorganizing the theoretical derivation process, we found that the inputs and outputs of the atomic and digital resonators are magnetization M and voltage U, respectively. The dimensional difference between them makes the subsequent derivation process not easy to follow. Therefore, we have added a nondimensionalization treatment for these physical quantities in the Supplementary materials to better understand the derivation process. More details of improvement are:

(i) We uniformly have used angular frequency ω to represent all frequency variables, $\Delta\omega$ to represent frequency differences, and ω_0 to represent the Larmor precession frequency of Xe atoms when the B_z input is 0 (approximately $2\pi \cdot 161.1\mathrm{Hz}$ in this paper).

(ii) We have added explanations for the coefficients k_1, k_2, g_1, and g_2 in both the main text and the Supplementary materials.

(iii) We have nondimensionalized the input and output physical quantities x and y in the Supplementary materials.

Revised content in the main text:

$\Delta\omega$ is the eigenfrequency difference between atoms and the digital resonator. ω_0 is the initial frequency of the system response when $\Delta B = 0$.

Next, as shown in Fig. 1(a), we linearly add their outputs and use the result as the system input, thus obtaining $x_n = g_n(\kappa_1 e^{-i\theta} y_1 + \kappa_2 e^{-i\varphi} y_2)$. Here $e^{-i\theta}$ and $e^{-i\varphi}$ are phase-shift factors and κ_1, κ_2, g_1, and g_2 are gain factors, all of which can be tuned in the computer simulation.

Revised content in the Supplementary materials:

To derive the system Hamiltonian $\hat{H}_{eff}$, we need the equations of motion for the atomic ensemble and the digital resonator separately. Assuming the Xe atoms are in a static magnetic field B_z, their motion can be described by the Bloch equation:

$$\dot{\vec{\boldsymbol{M}}} = \vec{\omega} \times \vec{\boldsymbol{M}} - \frac{M_x}{T_2}\vec{x} - \frac{M_y}{T_2}\vec{y} + \frac{M_0 - M_z}{T_1}\vec{z}, \tag{1}$$

here, $\vec{\boldsymbol{M}}$ is the atomic polarization vector, and $\vec{\omega}$ is the Larmor precession angular velocity. In a magnetic field, $\vec{\omega} = \Gamma\vec{B}$, where Γ is the gyromagnetic ratio. $M_{x(y,z)}$ denotes the component of $\vec{\boldsymbol{M}}$ along the $x(y,z)$ axis, and M_0 is the magnitude of M_z at steady state. T_2 and T_1 are the transverse and longitudinal relaxation times, respectively. In this experiment, the probe light propagates along the y-axis. It interacts with Rb atoms to get their precession signal, and then extracts the signal of Xe atoms ($M_{x(y)}$) through signal demodulation. Since we measure $M_{x(y)}$, we only need to consider the effect of T_2.

Expanding $\vec{\boldsymbol{M}}$ in the Bloch equation (1) along the x, y, and z axes respectively, we obtain the following equations:

$$\dot{M}_x = \omega_y M_z - \omega_z M_y - \frac{M_x}{T_2}, \tag{2}$$

$$\dot{M}_y = \omega_z M_x - \omega_x M_z - \frac{M_y}{T_2}, \tag{3}$$

$$\dot{M}_z = \omega_x M_y - \omega_y M_x - \frac{M_0 - M_z}{T_1}. \tag{4}$$

By introducing $M_+ = M_x - iM_y = M_\perp \cdot e^{i\varphi}$ in equations (2)-(4) and separating the imaginary and real parts, we can derive the following:

$$\dot{M}_+ = (\omega_y + i\omega_x)M_z - \left(i\omega_z + \frac{1}{T_2}\right)M_+. \tag{5}$$

In equation (5), M_y lies in the xy-plane and is 90° out of phase with M_x. Thus, we can denote $y_1 = \frac{M_+}{M_u}$ as the signal output, and $x_1 = \frac{M_z\omega_x}{M_u\omega_u} = \frac{M_z\Gamma B_x}{M_u\omega_u}$ as the signal input caused by the magnetic field B_x from the x-axis coil. Here M_u and ω_u represent unit magnetization and unit angular frequency, respectively, which make the system input x_1 and output y_1 dimensionless numbers. This operation not only preserves the correctness of the theoretical derivation but also greatly simplifies subsequent derivation processes. It is worth noting that after nondimensionalizing the input and output, parameters such as angular frequency ω and relaxation time T_2 in the equations become unitless.

Then, we use $\omega_z = \omega_1$ as the eigenfrequency of atomic precession, $\frac{1}{T_2} = \gamma_1$ as the atomic resonance loss, and $\omega_y = 0$ signifying no input along the y-axis. Assuming M_z remains constant during the experiment, equation (5) can be rewritten as follows.

$$\dot{y}_1 = -(i\omega_1 + \gamma_1)y_1 + ix_1. \tag{6}$$

The output signal y_1, derived from equation (6), is an oscillating signal of the form $M_\perp cos(\omega_1 + \phi_0)$, where ϕ_0 is the initial phase, ω_1 is the oscillation frequency, and $M_\perp$ is the signal amplitude. The loss γ_1 and input x_1 in equation (6) determine the variation of $M_\perp$. For subsequent discussion and calculation, y_1 continues to represent the output of the AM unit.

Similarly, for the digital resonator, we can derive an analogous equation of motion, which is also governed by a second-order differential equation:

$$\ddot{y}_2 + 2\gamma_2\dot{y}_2 + \omega_2^2 y_2 = 2\gamma_2\omega_2 x_2, \tag{7}$$

here, $x_2$and y_2 represent the input and output, ω_2 is the eigenfrequency, and γ_2 is the loss. For the digital resonator, both the input and output are voltage U. Their nondimensionalization is similar to that of the AM unit, requiring only division by the unit voltage U_u, which will not be discussed in detail here. Assuming the output signal is oscillatory, expressed as $y_2 = Ae^{-i\omega_2 t}$ (A is the signal amplitude), substituting this into equation (7) and neglecting the slow-varying term $\ddot{A}e^{-i\omega_2 t}$, we obtain:

$$-2i\omega_2\dot{A}e^{-i\omega_2 t} - \omega_2^2 Ae^{-i\omega_2 t} + 2\gamma_2\dot{A}e^{-i\omega_2 t} - 2i\omega_2\gamma_2 Ae^{-i\omega_2 t} + \omega_2^2 Ae^{-i\omega_2 t} = 2\gamma_2\omega_2 x_2. \tag{8}$$

After simplification, the equation (8) becomes:

$$\dot{y}_2 = -(i\omega_2 + \gamma_2)y_2 + \frac{\gamma_2^2}{\omega_2}x_2 + i\gamma_2 x_2. \tag{9}$$

Given that $\omega_2 \gg \gamma_2$, the term $\frac{\gamma_2^2}{\omega_2}x_2$ can be neglected. After normalizing the input term with respect to γ_2, equation (9) simplifies to:

$$\dot{y}_2 = -(i\omega_2 + \gamma_2)y_2 + ix_2, \tag{10}$$

whose form is identical to equation (6). Finally, they can be transformed into a Schrödinger-like form:

$$i\dot{y}_{1,2} = \left(\omega_{1,2} - i\gamma_{1,2}\right)y_{1,2} - x_{1,2}. \tag{11}$$

Experimentally, above dimensionless operation depends on linear mutual conversion between atomic magnetization and voltage signal.

In our system, we use the built-in Rb magnetometer to measure the magnetization M_{Xe} of Xe. First, Rb atoms can sense the weak magnetic field B_{Xe} generated by Xe atoms through spin-exchange collisions. Then, when the probe light passes through the cell and interacts with Rb, the detected signal carries the information of Xe. Subsequently, a balanced detector is used to receive the probe light, converting the optical signal into a voltage signal. Finally, by demodulating the signal, the signal of Xe can be separated, completing the detection of Xe magnetization. In this process, M_{Xe} has a linear relationship with the final output voltage U_1, i.e., $M_{Xe} \propto U_1$.

Similarly, the output signal of the digital resonator is voltage U_2, this voltage signal is first converted by the coil (assuming the coil constant is α, and in this paper $\alpha = 1.26\ \mathrm{nT/mV}$):

$$B_x = \alpha U_2. \tag{14}$$

Then through the interaction between magnetic field B_x and atoms (equation (5)), it is finally converted into atomic magnetization M_{Xe}. In summary, a linear conversion between the input and output of the AM and DE units can be achieved, which provides the necessary conditions for our subsequent derivations and experimental operations.

By setting the inputs as a linear combination of the output signals, specifically $x_{1,2} = g_{1,2}(\kappa_1 e^{-i\theta} y_1 + \kappa_2 e^{-i\varphi} y_2)$, we can derive the Hamiltonian matrix:

$$\hat{H}_{eff} = \begin{bmatrix} \omega_1 - i\gamma_1 - g_1\kappa_1 e^{-i\theta} & -g_1\kappa_2 e^{-i\varphi} \\ -g_2\kappa_1 e^{-i\theta} & \omega_2 - i\gamma_2 - g_2\kappa_2 e^{-i\varphi} \end{bmatrix}, \tag{15}$$

where $e^{-i\theta}$ and $e^{-i\varphi}$ are phase shifts caused by signal transmission delay, and we can achieve arbitrary regulation of the phase shift from 0 to 2π through hardware. $g_{1,2}$ and $\kappa_{1,2}$ are gain factors, which can be adjusted in magnitude according to the actual situation in the experiment.

Comment #6:

Figures: Fig. 1: In Fig. 1b the y-label is 'Non-EP response' which I presume should be the frequency of Xe, but is unclear. The x-axis is v, which is strange to use as this is the detuning between the frequency of the digital resonator and the Larmor frequency of Xe, so presumably this should just be the Larmor frequency of Xe. In Fig. 1c the y-axis should again be frequency of the Xe and frequency of the digital resonator. The fact it's not written like this makes it difficult to understand what's happening in the graphs.

Response #6:

Thank you for your nice suggestion, according to which we have provided more details and explanations for Figures 1c and 1d. We have defined the x-axis as the eigenfrequency difference $\Delta\omega$ between the two resonators and the y-axis as the output frequency of them.

The revised Figure 1 is shown below (We only revised the axes of Figure 1b-d, and added the explanation of $\Delta\omega$ and ω_0 in the caption (red-marked). The other parts are exactly the same as the original version):

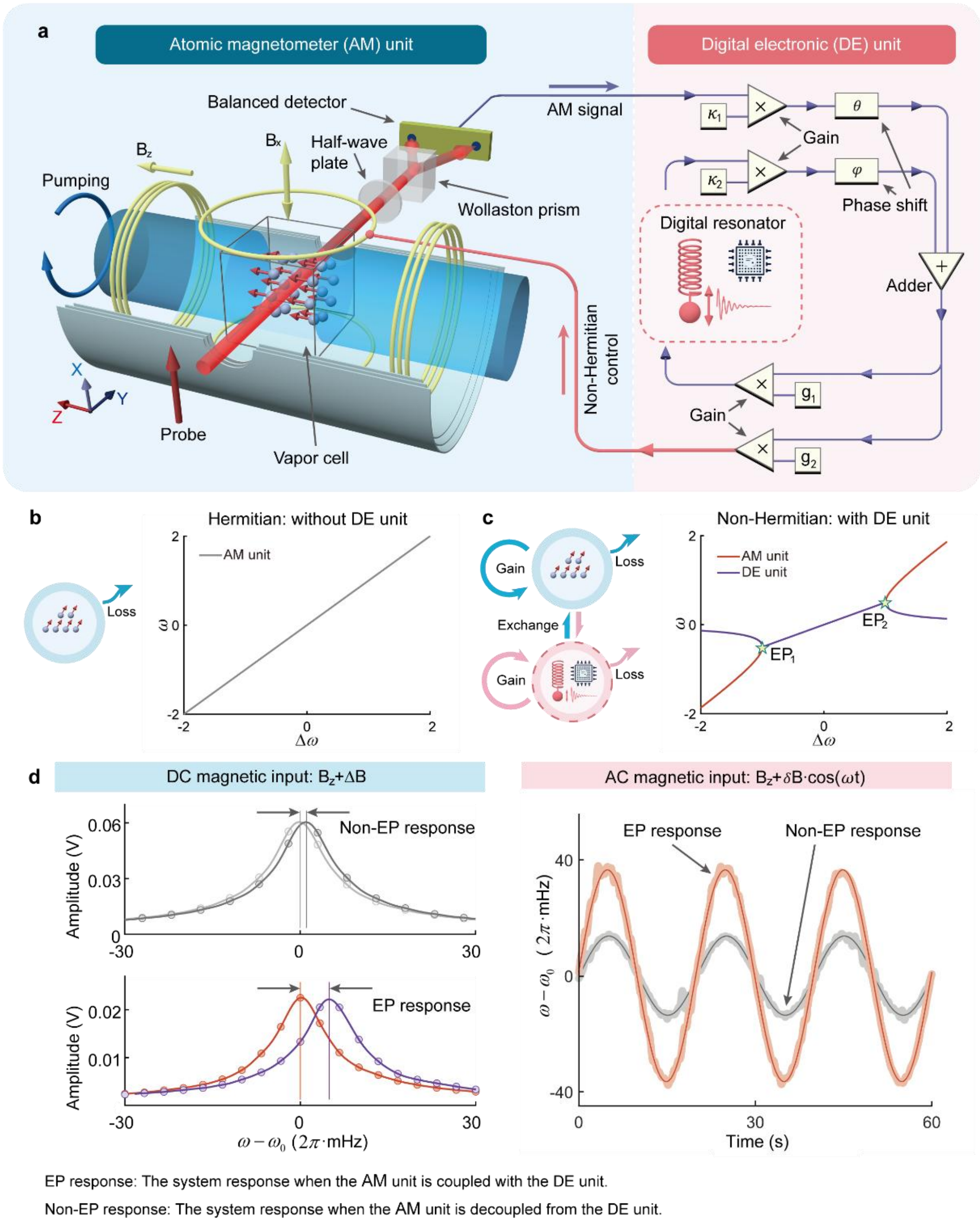

Fig. 1 | Hybrid EP-enhanced magnetometer with a DE unit. a, Schematic of the hybrid EP-enhanced magnetometer, consisting of an AM unit and a DE unit. The AM unit includes an atomic vapor cell, pump light, probe light, magnetic field coils, and detector. The DE unit is composed of a digitally simulated resonator and gain and phase shift modules. The gain module is implemented by a multiplier, the phase shift module is implemented by a shift register, and the signal coupling is performed by an addition operation. The atomic precession signal and the digital resonator signal are routed through the gain and phase shift modules and then coupled via an adder. The coupled signal is fed back to both the digital resonator and the atoms. **b, c** Simplified model of the hybrid non-Hermitian system and the response before and after coupling. After the AM unit couples with the DE unit, its linear response becomes an EP-enhanced response, with maximum enhancement near the EPs (as indicated by the stars); $\Delta\omega$ is the eigenfrequency difference between atoms and the digital resonator. **d,** Experimental results of the system response. The left figure illustrates the response of the AM and the EP-enhanced magnetometer to changes in the DC magnetic field ΔB. ω_0 is the initial frequency of the system response when $\Delta B = 0$. The right figure shows a comparison of their responses to an AC-modulated magnetic field signal $\delta B \cdot \cos(\omega t)$.

Comment #7:

The graphs in Fig. 1d make more sense. It shows that the Xe co-magnetometer is more sensitive to shifts of DC magnetic fields. This nicely shows how near the exceptional point the Xe is more sensitive to magnetic fields. The purpose of the data in Fig. 1d(ii) is unclear, as it seems to show the same effect as in Fig. 1(d).

Response #7:

In Figure 1d, the left panel shows the measurement results for the DC signal, while the right panel shows those for the AC signal. Our intention in presenting the data this way was to showcase the sensing advantages of our system to readers through comprehensive experimental results. We believe that bandwidth is also a crucial metric for atomic magnetometry, so displaying only DC signal measurements would not fully demonstrate its sensing capabilities.

Comment #8:

Fig. 2: In Fig. 2(a) the signal should not be a FID- instead it should be a sine wave as this is in the feedback configuration.

Response #8:

Thank you again for raising a critical question. In the dual-EP state, when the feedback strength does not exceed 1, which is the experimental condition in this paper, the system remains in a lossy attenuation state rather than a self-oscillation state. In the single-EP state, however, the loss is not affected by feedback and remains γ. Therefore, the signal remains a damped sinusoidal one. To address your confusion, we have added more explanations in the Supplementary materials, showing the variation of the system loss at the EPs.

Revised content in the Supplementary materials:

In the main text of this article, we extensively discussed the changes of the real part of eigenvalues. Here we supplement the explanation of the imaginary part of the system, i.e., the loss changes. Similar to the treatment in the manuscript, we first perform normalization processing on the coefficients in the Hamiltonian, setting $\kappa_1 = \kappa_2 = 1$, $g_1 = g_2 = g_0$ and $\gamma_1 = \gamma_2 = \gamma_0$.

In the case of dual-EP state ($\theta = \pi/2$ and $\varphi = \pi/2$), the eigenvalues are $\lambda = i(g_0 - \gamma_0) \pm \sqrt{\Delta\omega^2 - {g_0}^2}$. At the EPs, the imaginary part of the eigenvalue is $Im(\lambda)_{EP} = g_0 - \gamma_0$. Therefore, the system loss increases as the gain coefficient g becomes larger, and when $g_0 = \gamma_0$, the system loss drops to 0. As g_0 becomes larger, the signal strength also continuously increases, and the system's nonlinear effects continuously strengthen, which is detrimental to experimental measurement. Whereas when g_0 is too small, the system's coupling strength decreases, and the degeneracy interval width between EPs decreases, which is detrimental to observation and regulation. Therefore, in the dual-EP state, we choose to control g_0 at around $\gamma_0/2$, in order to balance excluding the influence of nonlinear effects and experimental regulation.

In the single-EP state, however, the system eigenvalue is $\lambda = -i\gamma_0 \pm \sqrt{\Delta\omega^2 + 2ig_0\Delta\omega}$, and its imaginary part is always equal to $-\gamma_0$. Therefore, regardless of the magnitude of g_0, the system loss remains unchanged, and the system's output signal is always a decaying sinusoidal signal. This shows that in the single-EP state, the system does not produce nonlinear effects due to feedback enhancement, which is one of the reasons why we ultimately chose to enhance sensing in this state.

Comment #9:

Fig. 2(b) is very confusing, as the x-axis seems to be centred around 100mHz. Presumably this data was taken with a bias field of 161.1Hz, and therefore this should either be centred around 161.1Hz (which I think is easier for the reader), or it should be centred around 0Hz if is along the x-axis.

Response #9:

We acknowledge that the issue you raised indeed exists, and this is one of the oversights in our work. As per your suggestion, we have changed the x-axis in the figure to the $\omega - \omega_0$ format, which allows for a clearer presentation of the experimental results.

The revised Figure 2 is shown below (We only revised the axes of Figure 2b-d, and added the explanation of Voltage U in the caption (red-marked). The other parts are exactly the same as the original version):

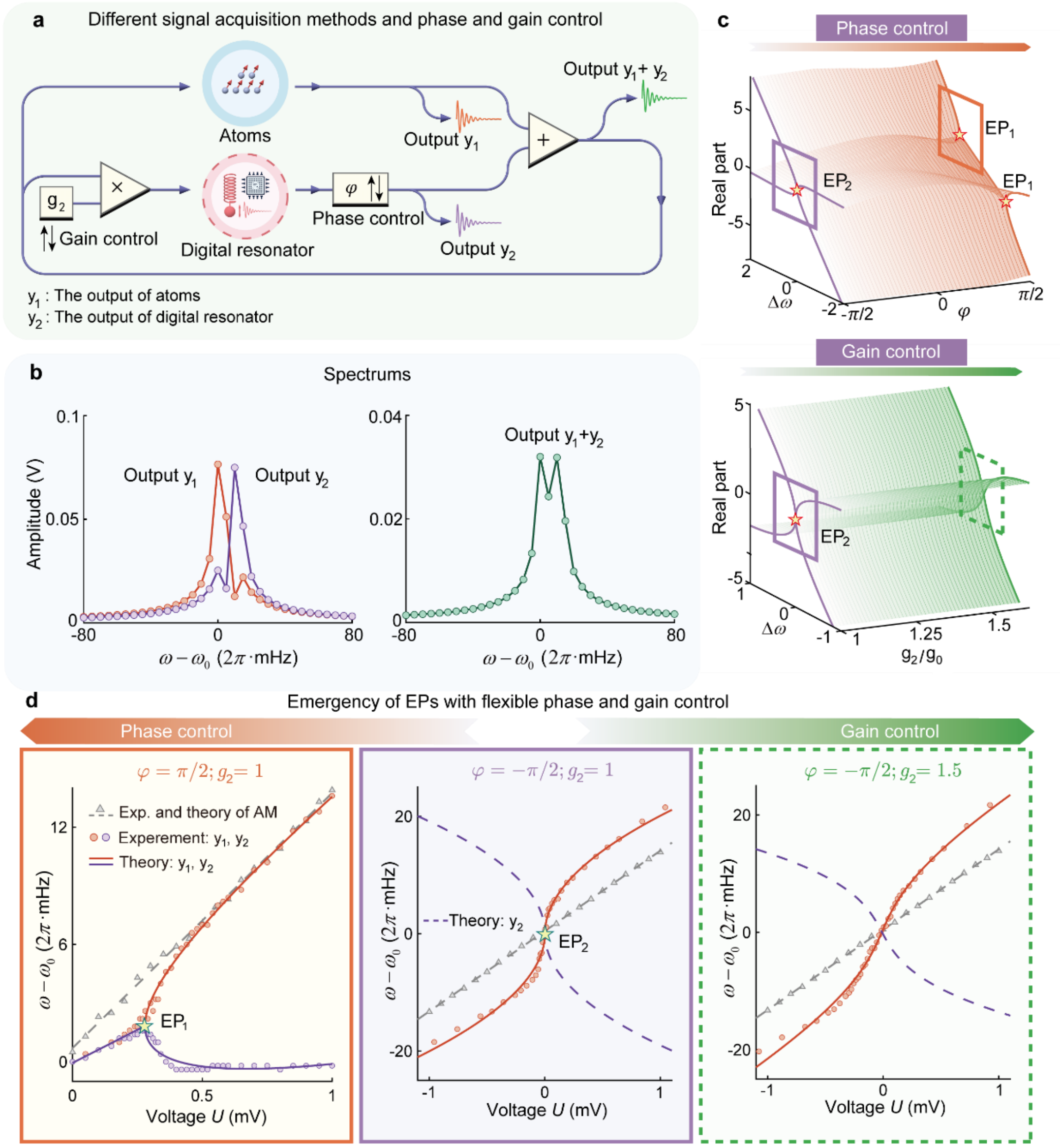

Fig. 2 | Flexible control of the hybrid non-Hermitian magnetometer. a, Control and signal extraction procedure for our hybrid non-Hermitian system. The system control consists of gain g_2 and phase φ. The hybrid system can simultaneously acquire three signals: the atomic signal y_1, the digital resonator signal y_2, and the combined signal $y_1 + y_2$, through separate ports. **b,** The Fourier spectra of the system output signal. The mutually independent data ports of the digital electronics can be used to separately extract signals from the magnetometer and the digital resonator or to extract the total signal. **c,** Dependence of the real parts of the eigenvalues on the phase shift φ and the gain module g_2. **d,** Experimental results for φ and g_2 control. The gray triangles represent the signal of the conventional AM, while the orange circles correspond to the magnetometer signal y_1 in the EP-enhanced magnetometer, and the purple circles represent the signal of the digital resonator y_2. The scatter points are experimental signals, and the curves are fits to data. The relationship between the voltage and the magnetic field is $B = 1.26\ \mathrm{nT/mV} \cdot U$.

Comment #10:

I don't really understand the relevance of Fig. 2b(ii), as the Xe atoms are the sensor and therefore it is not clear to me why the addition is shown.

Response #10:

Here we demonstrate the characteristics and advantages of this system for data acquisition and processing. We believe this approach can better illustrate the advantages of the DE unit in constructing non-Hermitian systems, while presenting the experimental details of data acquisition will also enable readers to more easily reproduce the work presented in this paper. Since very few previous studies have used digital electronics to investigate non-Hermitian problems, most people have found it difficult to appreciate the convenience that digital electronics bring to data acquisition and processing. We hope that this paper can open up new avenues of thinking for more readers through this approach.

Comment #11:

The graphs in Fig. 2(d) are important and nicely done. The graphs show that Xe becomes more sensitive to magnetic fields, i.e. bigger frequency shift for small change in bias field. The theory and experiment overlap. But Voltage U(mV) is undefined in the text- I presume this is the current sent to the coil? Also, the y-axis should read frequency difference, or if it's frequency it should be 161.1 Hz. Parameters like g2, k2, U are used interchangeably without proper definitions.

Response #11:

Thank you for these good suggestions. Similar to the previous revisions, we have changed the x-axis in Figure 2 to the $\omega - \omega_0$ format, performed non-dimensionalization of the input x and output y, and provided more detailed explanations for the gain coefficients k_1, k_2, g_1, and g_2. Furthermore, we have explained the relationship between voltage and magnetic field in the figure caption, making the figure content clearer and more explicit.

Comment #12:

Lack of experimental details: The fact that the makeup of the vapour cell (Rb, Xe, N2?) is not included until the methods section is a big omission. Is there buffer gas in the Xe/Cs cell? What is the pressure in the cell? Move essential details of experimental setup (nitrogen pressure, Xe129 pressure, cell temperature, DE settings) into main text. No details are given about the DE package. Is this a DDS or FPGA? What settings are used? There is no chance for the reader to replicate what has been shown here experimentally. I would strongly encourage the authors to think about all the details that would be necessary to replicate this experiment, including lasers used (transition, powers) etc.

Response #12:

Thank you for pointing out this issue. We have referred to the writing styles of other articles and added experimental details according to the standard that readers should be able to reproduce the results. These details include laser parameters, atomic composition and pressure in the gas cell, experimental temperature, coil constants, and software and hardware information of the DE unit.

Revised content in the main text:

The atoms are enclosed in a spherical glass vapor cell with a diameter of about 8 mm, containing 10 Torr of ^{129}Xe, 300 Torr of buffer gas N_2, and an excess of saturated Rb metal. During the experiment, the vapor cell is kept at 105 °C.

The pump light has a power of 35.52 mW and a wavelength of 795 nm, corresponding to the D1 line of Rb atoms. The probe light has a power of 1.05 mW and a wavelength of 780 nm, which is detuned by 40 GHz from the D2 line of Rb atoms.

We use the first-order Butterworth band-pass filter module in LabVIEW to implement the digital resonator. This module can readily simulate the signal and response of the resonator, and by changing the bandwidth and center frequency we can correspondingly vary the loss and eigenfrequency of the digital resonator. In the experiment, a 7856R FPGA board is additionally used for sampling, with a sampling rate of 500 kHz.

Comment #13:

Missing key citation: 'Stable Atomic Magnetometer in Parity-Time Symmetry Broken Phase, Phys. Rev. Lett. 130, 023201 (2023)'. This is a great example of a paper where PT symmetry breaking is demonstrated in Xe129. They do systematic measurements of how magnetic field gradients induce PT symmetry breaking in Xe129- the mechanism for how PT symmetry is broken is very clear, and is a good example of the clarity the authors should be aiming for in this paper.

Response #13:

After reading and studying this paper, we believe that the authors achieved remarkable non-Hermitian effects in atomic spin systems through magnetic gradient control, and achieved higher-sensitivity rotation measurements on this basis. We have added citations to the main text as you suggested.

List of main changes

Main changes in the main text

(i) Page 3, Fig. 1, we revised the figure for more clear axis definition.

(ii) Page 4-5, we added more theoretical derivation details.

(iii) Page 6, Fig. 2, we updated the axis definition, and added explanation of the relationship between voltage and magnetic field.

(iv) Page 7, 4th paragraph, we clarified the relationship between SNR and sensitivity.

(v) Page 9, Last paragraph, we added discussion on the application prospects of this work.

(vi) Related references have been added as Refs. [3, 14, 32].

Main changes in the Methods and Supplementary materials

(vii) Methods, Atomic magnetometer (AM) unit, we added necessary experimental details.

(viii) Methods, Digital electronic (DE) unit, we added hardware and software information.

(ix) Methods, Phase and gain control, we added discussion of system when $g_2/g_0 < 1$.

(x) Methods, Noise analysis, we added more discussion on noise sources.

(xi) Supplementary materials, Complete Hamiltonian, we added the nondimensionalization derivation process, and added the conversion relationship between magnetization and voltage.

(xii) Supplementary materials, The loss of the hybrid system, we added discussion on losses.

(xiii) Supplementary materials, SNR and sensitivity, we explained in detail the relationship between SNR and sensitivity, and provided the calculation method for sensitivity.